

To appear in ApJ., XXX

Evidence for Granulation and Oscillations in Procyon from Photometry with the WIRE satellite

H. Bruntt

*Niels Bohr Institute, University of Copenhagen, Juliane Maries Vej 30, DK-2100
Copenhagen Ø, Denmark*

`bruntt@phys.au.dk`

H. Kjeldsen

*Department of Physics and Astronomy, University of Aarhus, Ny Munkegade, Bygn. 520,
DK-8000 Aarhus C., Denmark*

`hans@phys.au.dk`

D. L. Buzasi

US Air Force Academy, Department of Physics, CO, USA

`Derek.Buzasi@usafa.af.mil`

T. R. Bedding

School of Physics, University of Sydney, Australia

`T.Bedding@physics.usyd.edu.au`

ABSTRACT

We report evidence for the granulation signal in the star Procyon A, based on two photometric time series from the star tracker on the WIRE satellite. The power spectra show evidence of excess power around 1 mHz, consistent with the detection of p-modes reported from radial velocity measurements. We see a significant increase in the noise level below 3 mHz, which we interpret as the granulation signal. We have made a large set of numerical simulations to constrain the amplitude and timescale of the granulation signal and the amplitude of the oscillations. We find that the timescale for granulation is $\Gamma_{\text{gran}} = 750 \pm 200$ s, the

granulation amplitude is 1.8 ± 0.3 times solar, and the amplitude of the p-modes is 8 ± 3 ppm. We found the distribution of peak heights in the observed power spectra to be consistent with that expected from p-mode oscillations. However, the quality of the data is not sufficient to measure the large separation or detect a comb-like structure, as seen in the p-modes of the Sun. Comparison with the recent negative result from the MOST satellite reveal that the MOST data must have an additional noise source that prevented the detection of oscillations.

Subject headings: stars: individual(Procyon), stars: granulation, stars: oscillations, stars: variable

1. Introduction

A clear signature of the transportation of heat by convection in the outer parts of the Sun is the convection cells or granules. The spatially and temporally incoherent signal generated by the granulation can be measured as background noise in the integrated light from the disk of the Sun. The physical phenomena on the surface give rise to noise in different frequency ranges. In order of increasing frequency, we find activity ($< 1 \mu\text{Hz}$), super-granulation ($< 10 \mu\text{Hz}$), meso-granulation ($< 100 \mu\text{Hz}$) and granulation ($2\,000 - 10\,000 \mu\text{Hz}$) (Harvey 1985; Aigrain et al. 2004).

There are several reasons why it is important to characterize granulation on other stars, apart from the obvious interest in testing models of convection. Although the solar five-minute oscillations ($\nu \simeq 3\,000 \mu\text{Hz}$) are detectable above the granulation noise, it is difficult to measure solar-like oscillations in stars with more vigorous surface convection. Also, the background noise at low frequencies ($< 200 \mu\text{Hz}$) is an important limiting factor when searching for the gravity modes in the Sun and other stars. Finally, the search for Earth-sized planets from space will also be affected by the background noise from large-scale granulation (Aigrain et al. 2004).

Evidence for granulation noise in two stars (α Cen A and Procyon A) was reported by Kjeldsen et al. (1999), based on measuring the equivalent widths of temperature-sensitive spectral lines. More recently, the MOST satellite (Walker et al. 2003) observed the F5IV type star Procyon A in early 2004 for 32 days with a duty cycle of 99% (Matthews et al. 2004). Since this star is more evolved and hotter than the Sun, the granulation is expected to be more vigorous and this was indeed what was reported by Matthews et al. (2004). The observed noise in the light curve obtained with MOST is four to five times higher than what is measured in the Sun in the frequency range 1-2 mHz (Bedding et al. 2005) and hampers the

detection of the p modes (Matthews et al. 2004). However, Bedding et al. (2005) have made simulations of the MOST time series and suggested that the noise signal seen by Matthews et al. (2004) is a combination of granulation and instrumental effects (e.g. scattered light).

In this study we have used two photometric time-series of Procyon A from the star tracker on the Wide-field Infrared Explorer satellite (WIRE). In Section 2 we describe the observations and data reduction procedure. In Section 3 we analyze the resulting power density spectra. In Section 4 we compare the observed power spectra with a grid of simulations in order to estimate the amplitude and timescale of the granulation and to constrain the amplitude of the p mode signal. In Section 5 we discuss our results.

2. Observations and Data Reduction

The star tracker on WIRE has a 52 mm aperture with a 512×512 CCD. A window of 8×8 pixels centered on the star image is integrated for 0.5 seconds and read out. The FWHM of the stellar image is around 1.8 pixels and thus is well sampled. The CCD image is not flat-fielded, so variations of sensitivity with position are expected. Fortunately, the pointing of the satellite is stable to about one hundredth of a pixel over periods of several days. Note that one pixel corresponds to about one arc minute.

WIRE observed Procyon in September/October 1999 and September 2000 for 9.5 and 7.9 days, respectively. Each of the two data sets consists of a few hundred thousand CCD images. Each WIRE observation consist of five 0.1 second integrations which are summed on-orbit by the firmware. Since the onboard electronics is 16-bit, when these five frames are summed for a bright target such as Procyon, saturation occurs, but this is only saturation in the sense that the data registers overflow and wrap when reaching $2^{16} = 65536$ ADU. Procyon is so bright that three of the central pixels reach the digital 16-bit maximum. Above this level the pixel value will start counting from zero. Thus we added 2^{16} to the central three pixels to account for this.

We have developed a new pipeline for the data reduction which differs significantly from our previous work on WIRE data (Buzasi et al. 2000; Schou & Buzasi 2001; Retter et al. 2003) and so we will describe it in some detail. For the background estimate we used 12 pixels (3 pixels in each corner of the CCD window). We fitted a Gaussian to each image to find the approximate position and FWHM of the image. For robustness, the background, position and FWHM used for each image were the means of 20 images taken before and after that image (while requiring that no image was separated in time by more than 30 seconds). Thus, we typically averaged these parameters over $41 \times 0.5 = 20.5$ seconds. We then performed

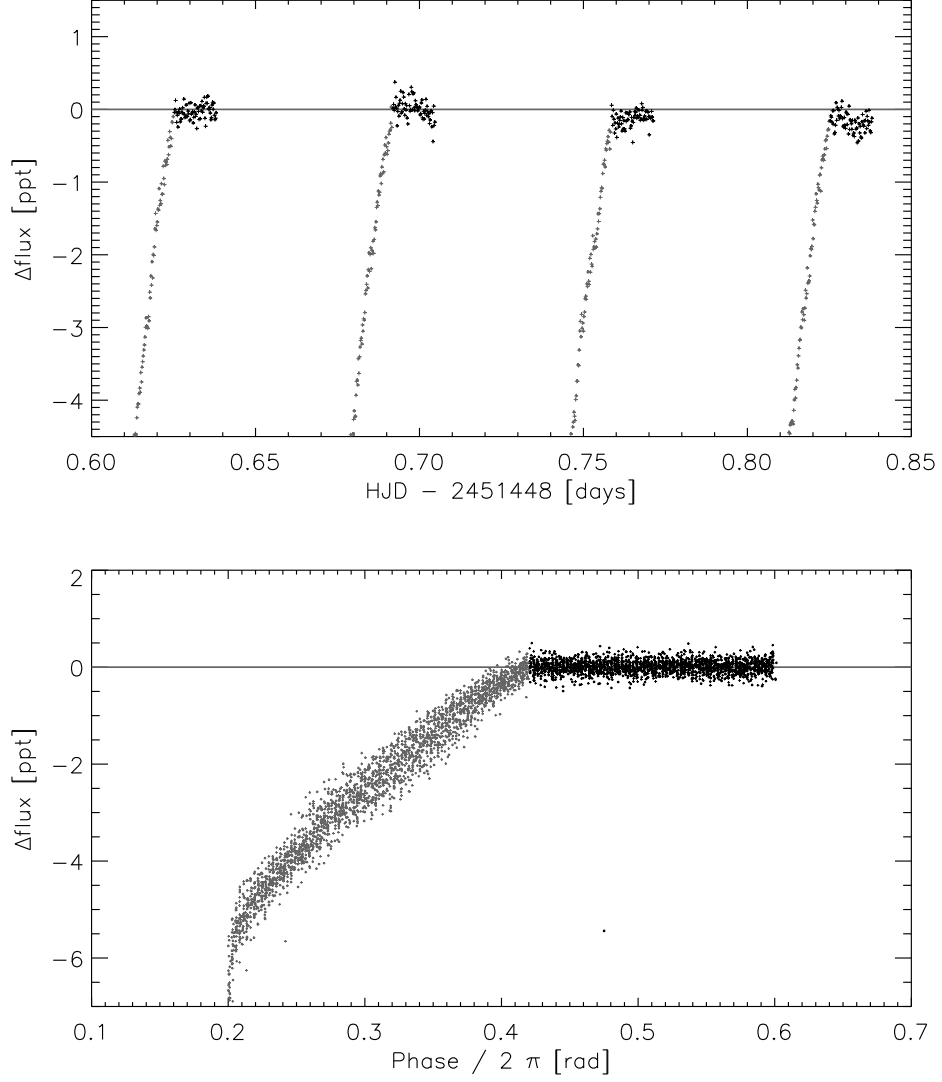


Fig. 1.— The *top* plot shows part of the raw light curve of Procyon from 1999. The gray data points at the beginning of each orbit of WIRE are affected by scattered light. The *bottom* plot shows the phased light curve (only every 20th data point in plotted). The gray points mark the points that are affected by scattered light and which were not used in the analysis.

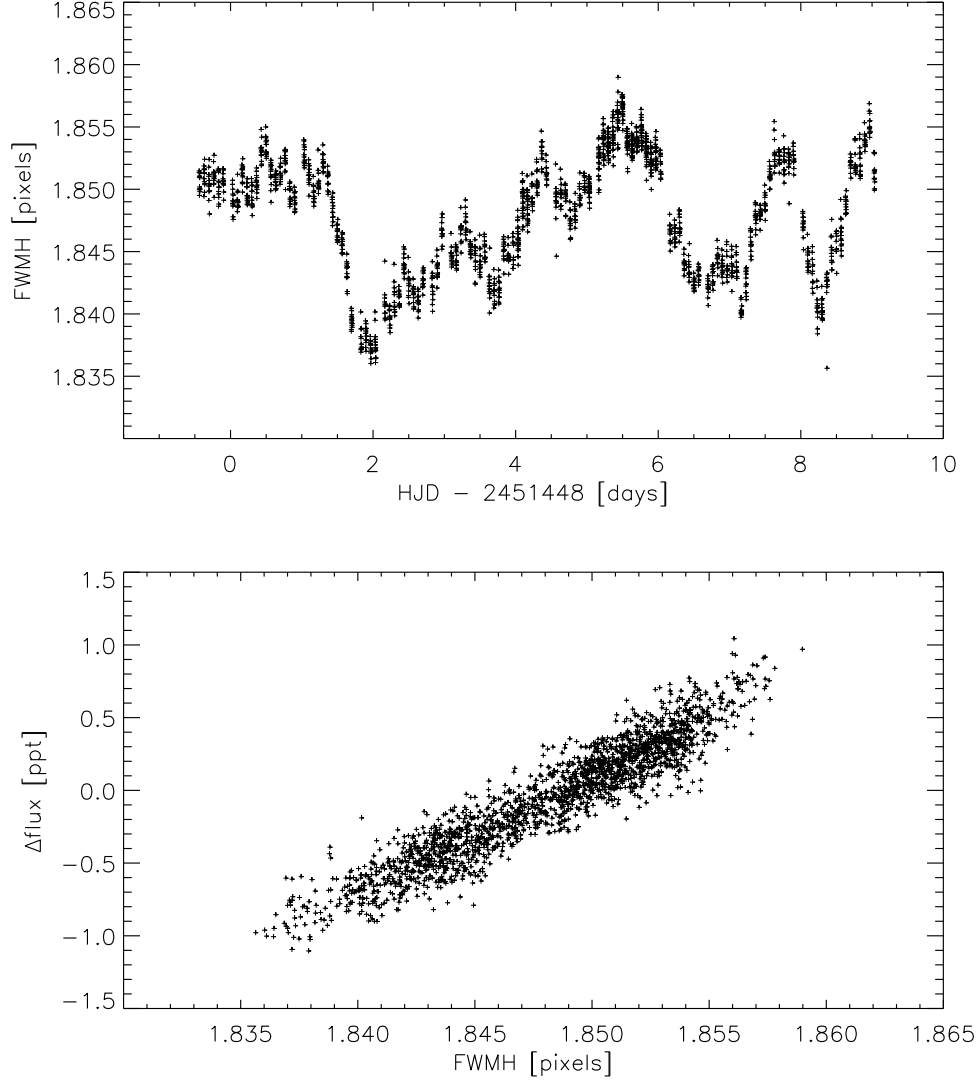


Fig. 2.— The *top* plot shows the change in the measured FWHM of the stellar profile versus time for the WIRE 1999 light curve. Only data points not affected by scattered light are plotted and only every 20th data point is plotted. In the *bottom* plot the flux change is plotted versus FWHM when using the same data points as in the *top* plot. There is a significant correlation which was taken out by a spline fit to the data points.

aperture photometry with nine increasing sizes, allowing us to select the one with the lowest intrinsic noise. The aperture sizes were scaled to the measured FWHM to include the same amount of light, independent of FWHM. However, the changes in FWHM for the Procyon observations were below 2% and so the actual number of pixels being summed did not vary. For the reduction of the Procyon data we summed 22 pixels.

For faster processing of the light curves, we binned data within every 15.5 seconds (i.e. 31 data points) which resulted in light curves from WIRE 1999 and 2000 series with 22 013 and 14 179 data points. In Fig. 1 we show the light curve from 1999 for four orbits. In the *top* panel the data are plotted versus time and in the *bottom* panel they are phased with the orbital frequency of 15.003 ± 0.001 c/day. The gray points are data affected by scattered Earth light. This is due to the fact that we underestimated the contribution of the background light and thus overestimated the brightness of the star. We have tried to remove the scattered light by fitting a spline to the phased light curve in Fig. 1 but the overall noise level is worse than if we just discard these data. Thus, the data affected by scattered light have been removed and the number of data points was then reduced to 10 610 and 8 397 for the WIRE 1999 and 2000 light curves.

In the case of the WIRE 1999 light curve we found that a group of data points taken around heliocentric Julian date 2451051.3 ± 0.4 days were offset by a significant amount, i.e. +3 ppt. We have found no correlation with any of our reduction parameters, e.g. FWHM, background level or orbital phase. This group of points contains 13% of the total data set and so, instead of rejecting them, we artificially offset these points to have the same median level as the rest of the dataset. We presume that this effect could be caused by one of the bits “sticking” in the ADC.

In Fig. 2 we show how the 1999 photometry correlates with the measured FWHM of the stellar profile. The *top* panel shows the FWHM changing slowly with time and the *bottom* panel shows flux versus FWHM. There is a significant correlation in the *bottom* panel, which we removed using a spline fit. A similar decorrelation procedure was carried out for the WIRE 2000 data.

2.1. Comparison of the WIRE and MOST time series

In Fig. 3 we show the final WIRE light curves of Procyon as observed in 1999 (*top* panel) and 2000 (*middle* panel). For comparison we also show part of the light curve observed by

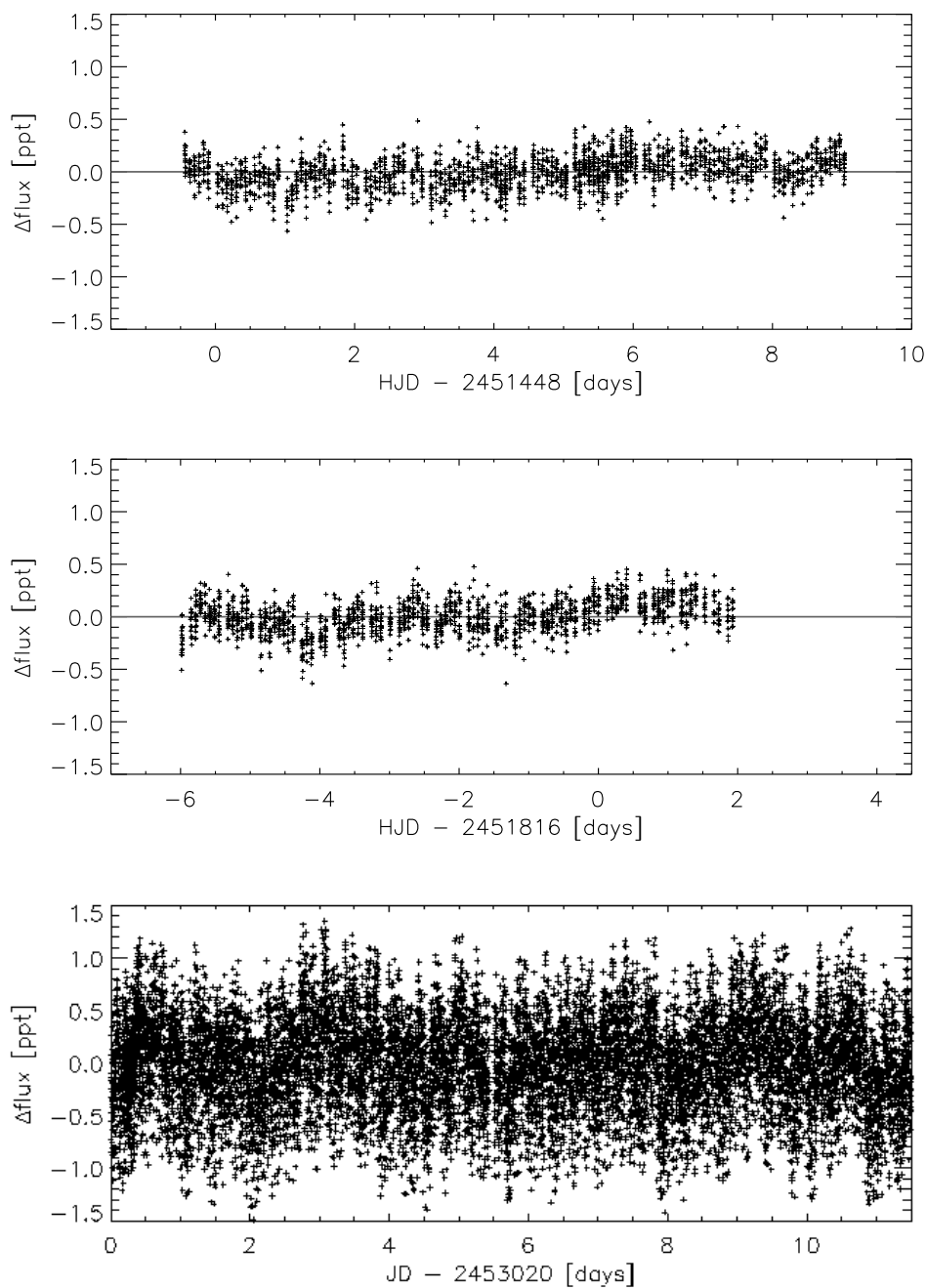


Fig. 3.— The final light curves of Procyon as seen from WIRE in September 1999 (*top*) and September 2000 (*bottom*). Data affected by scattered light has been removed and the correlation with FWHM has been removed. In each panel, only every fifth data point is plotted.

MOST in 2004¹. A slowly varying trend seen in the MOST light curve was subtracted. The same trend was also seen in a comparison star as shown by Matthews et al. (2004). During the first 20 days the MOST time series has a data point every 14.7 seconds which is part of the data shown in Fig. 3. This is very close to the cadence for the binned WIRE light curves which has one data point each 15.5 seconds. Note, however that the duty cycle is 18% in the WIRE datasets compared to 99% for the MOST dataset. In Fig. 3 only every fifth data point is plotted.

The values of *rms* noise in the 1999 and 2000 WIRE light curves are 135 and 129 ppm, and the point-to-point scatters (which measure high-frequency noise) are 105 and 101 ppm. The photon-noise limit for WIRE is 88 ppm, which is about 15–20% lower than the observed point-to-point scatter. The extra noise could be due to intrinsic variations in Procyon or instrumental effects. For MOST, the point-to-point scatter is 370 ppm and the photon-noise limit is 111 ppm, based on the mean flux level of 1.34×10^7 ADU (Matthews et al. 2004) and a gain of $6.1 e^-/\text{ADU}$ (Walker et al. 2003). Thus, the photon noise in the MOST data is a factor of 3.3 lower than the observed noise level. Note that the results of Matthews et al. (2004) were based on a preliminary data reduction and a more refined reduction gives slightly better results (J. Matthews & R. Kuschnig, private communication). We conclude that the MOST time series is affected by a noise source other than pure photon statistics, which was also suggested by Bedding et al. (2005) based on the distribution of peak heights in the amplitude spectrum.

We measured the white noise levels in the 1999 and 2000 WIRE amplitude spectra at frequencies between 8 and 10 mHz and found 1.8 and 1.9 ppm. Thanks to the much higher number of data points, the MOST amplitude spectrum has a noise level of 1.6 ppm in the same frequency range.

3. Power density analysis

To measure noise levels as a function of frequency in the different time series, we calculated power density spectra (PDS). Power density measures the power per frequency resolution element, which automatically makes it independent of the length (and sampling function) of the time series. We calculated the frequency resolution by measuring the area under the spectral window, which is the power spectrum of a single sinusoidal oscillation with an amplitude of 1 ppm that is sampled using the same times and weights as the observed series. These areas, which we used to convert from power to power density, were 7.29 and

¹The light curve was obtained at CADC through the MOST website: <http://www.astro.ubc.ca/MOST/>

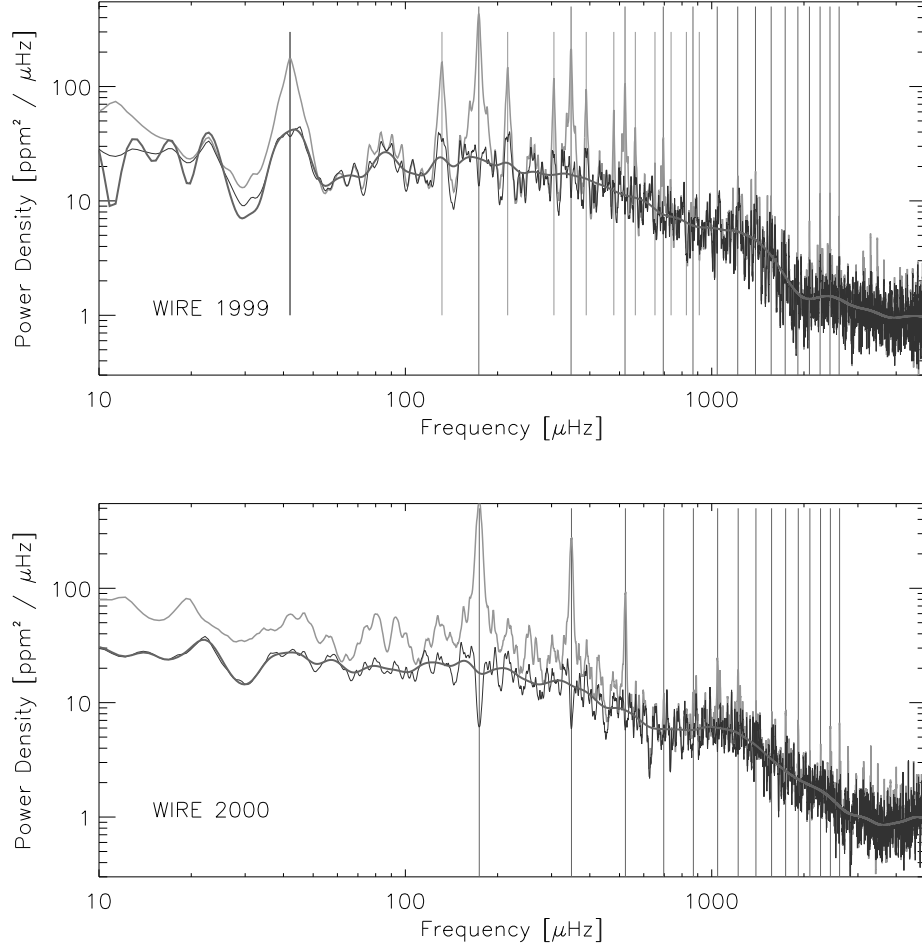


Fig. 4.— Power density spectrum of the WIRE 1999 (*top*) and WIRE 2000 (*bottom*) light curves. The gray curves are the original PDS and the black curve is the PDS after subtracting low frequency components. The smoothed version of the cleaned spectrum is also shown. The vertical lines mark integer multiples of the orbital frequency. For the WIRE 1999 light curve the combination frequencies of the peak at ~ 43 mHz are also marked.

7.02 μHz for the WIRE 1999 and 2000 light curves, respectively.

The WIRE light curves contain a number of significant outliers and to suppress their influence on the amplitude spectra we have computed weights for all points. Each point was a weight based on the scatter relative to the neighboring four data points (with the additional constraint that those data points must be within the same WIRE orbit). We then smoothed these weights using a running mean of width 150 data points.

The gray curve in each panel of Fig. 4 shows the PDS from WIRE for 1999 and 2000. There are a few peaks below 15 μHz (corresponding to periods longer than one day) which we do not attribute to the star. This low-frequency power generates aliases close to the harmonics of the orbital frequency of the WIRE satellite, around $n \times 174$ μHz , which are marked by vertical lines. In the case of the WIRE 1999 spectrum, we also see a power excess around 43 μHz that is not seen in the WIRE 2000 data. This excess also appears as aliases on either side of each orbital harmonic, as marked by additional vertical lines in the upper panel of Fig. 4.

We removed the low-frequency components from each light curve by the standard method of repeatedly subtracting the sinusoid corresponding to the strongest peak in the power spectrum. We removed three and four components from the WIRE 1999 and 2000 light curves, respectively, and so obtained the high-pass filtered PDS shown in black in Fig. 4. We can see that the excess power at the harmonics of the orbital frequency is greatly reduced. In each panel we have also over-plotted a smoothed version of the high-pass filtered PDS, and these are also shown in Fig. 5.

It can be seen in Fig. 4 that the high-pass filtered WIRE 1999 PDS still has some excess power at the orbital harmonic frequencies that is not seen in the WIRE 2000 PDS. This may explain the slightly higher level seen in the PDS of WIRE 1999 compared to WIRE 2000 in the 300–800 μHz range in Fig. 5.

In Fig. 5 we also compare the WIRE PDS with that from the MOST data. We calculated the frequency resolution of the MOST time series, as described above, to be 0.412 μHz , which is close to the theoretical value $10^6/(32 \cdot 0.99 \cdot 86400)$ $\mu\text{Hz} = 0.365$ μHz for a 32 day time series with a 99% duty cycle. From Fig. 5 we find that the noise level in the range 200–600 μHz in the WIRE data is a factor of 4 lower in power (2 in amplitude) compared to the MOST data.

In Fig. 5 we also show the power density spectrum based on VIRGO data (green channel) of the Sun (Fröhlich et al. 1997). The granulation signal in the Sun around 100–300 μHz is about a factor of two lower in power compared to the WIRE observations of Procyon. The bump seen at ~ 3 μHz is power from the solar p-modes.

When comparing observations, we must keep in mind that they were taken over different wavelength ranges. The MOST satellite has a broadband filter covering 350–700 nm, while the VIRGO green channel has a narrow band at 500 nm. The filter response of the WIRE star tracker is not known, but calibrations of the count levels observed in about 50 stars of different spectral type indicate that the filter response is more sensitive in the blue than in the red. We find the observed count levels observed with WIRE agree for both early and late type stars if the filter is Johnson *B*. Thus, the passbands of the MOST, VIRGO and WIRE spacecraft are roughly comparable.

4. Simulations of Procyon

We have made simulations of the granulation and p-modes in Procyon based on a software package developed to provide time-series simulations for the Danish MONS/Rømer satellite mission as well as for the ESA Eddington mission. We refer to Stello et al. (2004) for details of the simulations.

The simulation software has several parameters that can be modified. Firstly, we can set the white noise level in the simulations, which is determined by the noise level at high frequencies (above 8 mHz). For the granulation noise, we can change the timescale and granulation amplitude, while the p-modes are described by peak amplitude, lifetime and frequencies. The granulation signal seen in the PDS will depend on the input amplitude but also the time scale of the granulation. Thus, we use the measured granulation power density at low frequencies (20–120 μ Hz) from this point on. To include the p-modes in the simulation, we adopted a large separation of 55.5 μ Hz and a small separation of 4.9 μ Hz (e.g. Martić et al. 2004). We only included modes of degree $l = 0, 1$, and 2 and we have modified the amplitudes by a Gaussian envelope to emulate the signal seen in other sun-like stars. As an example, we show the distribution of the amplitude of the modes for peak amplitudes for the $l = 1$ modes of 8.5 ppm in Fig. 6.

4.1. Estimating the parameter range

To get an idea of the parameters that are needed to fit the observed PDS, and of the uncertainties in these parameters, we have made several simulations. In Fig. 7 we show results for the WIRE 2000 time series. In each panel, the observed spectrum is shown as a solid black line, and we adjusted the parameters in the following four steps.

The *top left* panel shows in gray two simulated PDS with white noise levels of 100

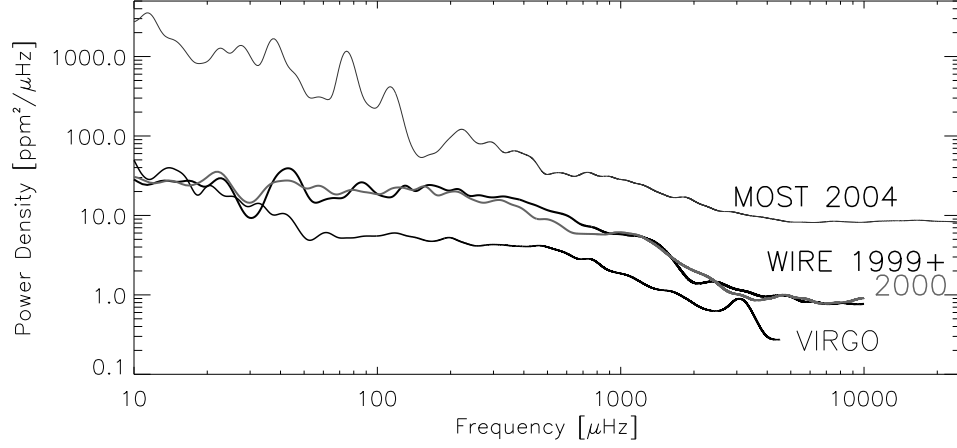


Fig. 5.— Smoothed PDS based on the MOST 2004, WIRE 1999 and 2000 data sets. The PDS based on VIRGO solar data from the green channel is shown for comparison.

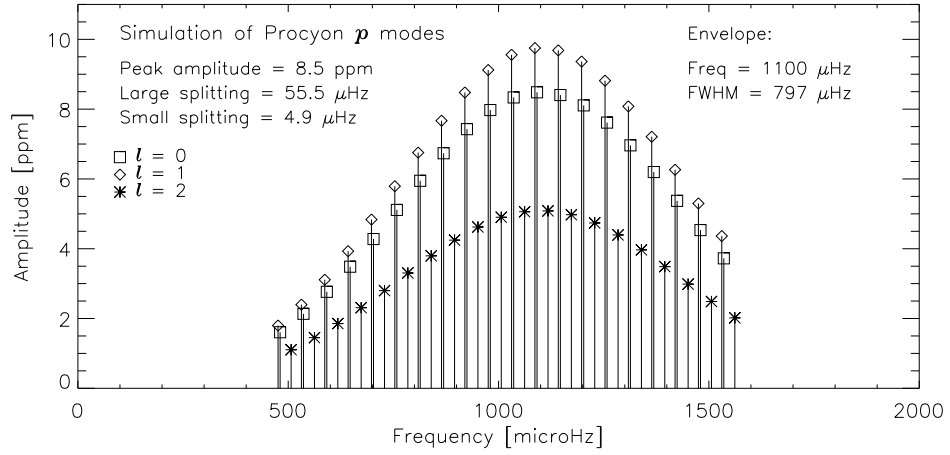


Fig. 6.— Input frequencies and amplitudes for the simulation of p-modes in Procyon.

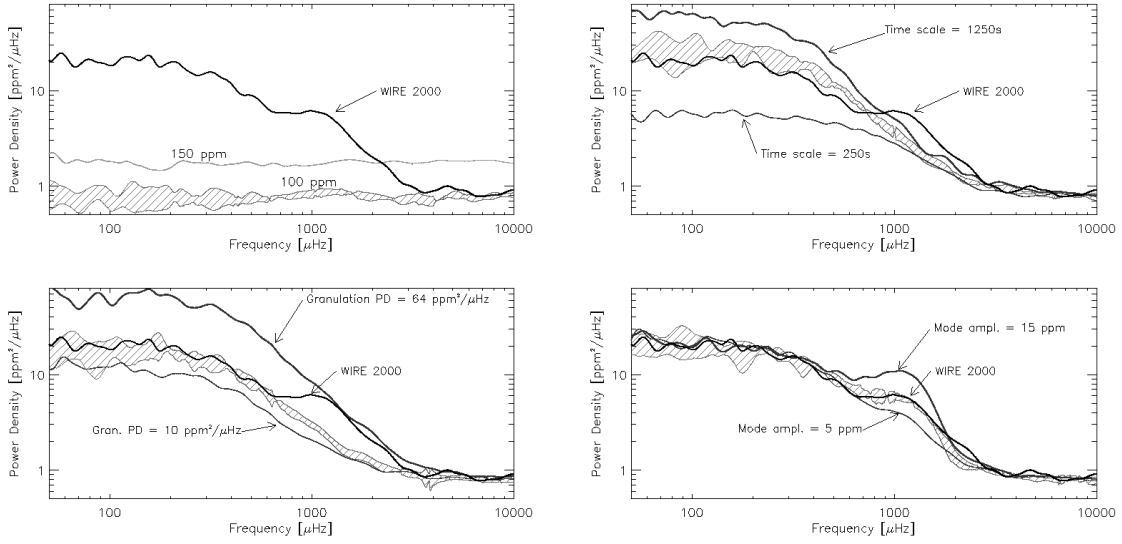


Fig. 7.— The four panels show the power density spectrum of the WIRE 2000 along with different simulations. Each simulation is the mean of five simulations with different seed numbers. The hatched regions show the $1\text{-}\sigma$ variation for selected simulations. In the *top left* panel simulations for two different white noise levels are shown. In the *top right* panel the simulations have timescales of the granulation of 250, 750, and 1250 s. In the *bottom left* panel the timescale of the granulation is 750 s but the granulation power densities (PDs) are 10, 18, and 64 $\text{ppm}^2/\mu\text{Hz}$. In the *bottom right* panel the granulation timescale and granulation PDs are 750 s and 18 $\text{ppm}^2/\mu\text{Hz}$, while the amplitude of the p-modes are 5, 10, 15 ppm.

and 150 ppm, respectively. In this and all other panels, the hatched region shows the $1\text{-}\sigma$ variation, which was found from five simulations that differed only in the seed for the random-number generator. For clarity, this $1\text{-}\sigma$ variation is only shown for one of the cases. Based on this panel, we have fixed the white noise at 100 ppm for the remaining three panels.

In the *top right* panel we have now added granulation with three different timescales: 250, 750 and 1250 seconds. These simulations allow us to rule out timescales lower than 250 s, based on the frequency at which the slope changes. For the next two panels, we have fixed the granulation timescale at 750 s.

In the *bottom left* panel, having fixed the white noise and the granulation timescale, we now show the PDS for three different granulation levels: 10, 18, and 64 $\text{ppm}^2/\mu\text{Hz}$. Note that the granulation power density is measured at low frequencies, i.e. below 120 μHz .

Finally, in the *bottom right* panel we retain the previous parameters and fix the granulation level at 18 $\text{ppm}^2/\mu\text{Hz}$. We now add p-mode oscillations with three different peak amplitudes: 5, 10, and 15 ppm. We adopted a mode lifetime of 1 day but note that, given the way the PDS are smoothed, the results are not affected by changing this value.

Our simulations are able to fit the observed power density spectrum quite well. Based on Fig. 7 we can conclude that the white noise level is about 100 ± 5 ppm, the granulation timescale must be larger than 250 s and probably less than 1250 s, the granulation PD must lie around 18 ± 5 $\text{ppm}^2/\mu\text{Hz}$ while the peak amplitude of the p-modes must certainly be less than 15 ppm.

4.2. Constraining the simulation parameters

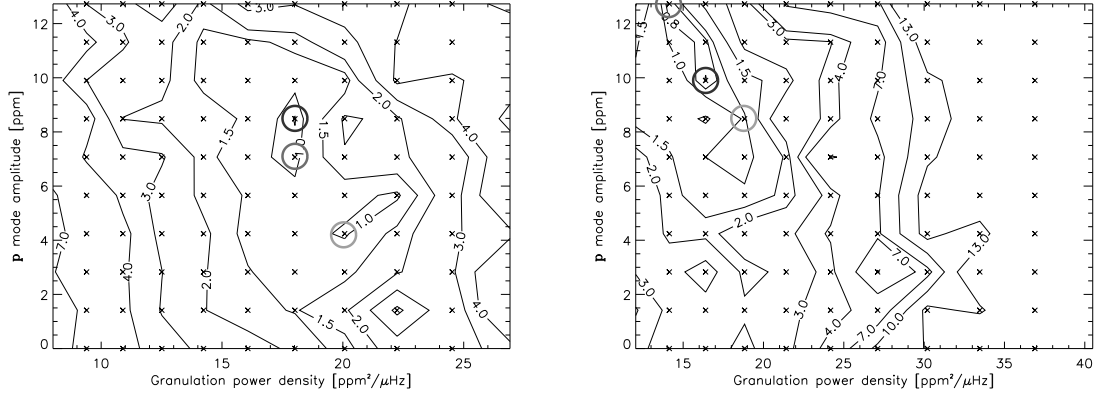


Fig. 8.— The two panels show contours of the χ^2 for the comparison of the WIRE 2000 and simulation power spectra with different values for the granulation PD and p-mode amplitude. The granulation time scales are 500 (*left* panel) and 750 seconds.

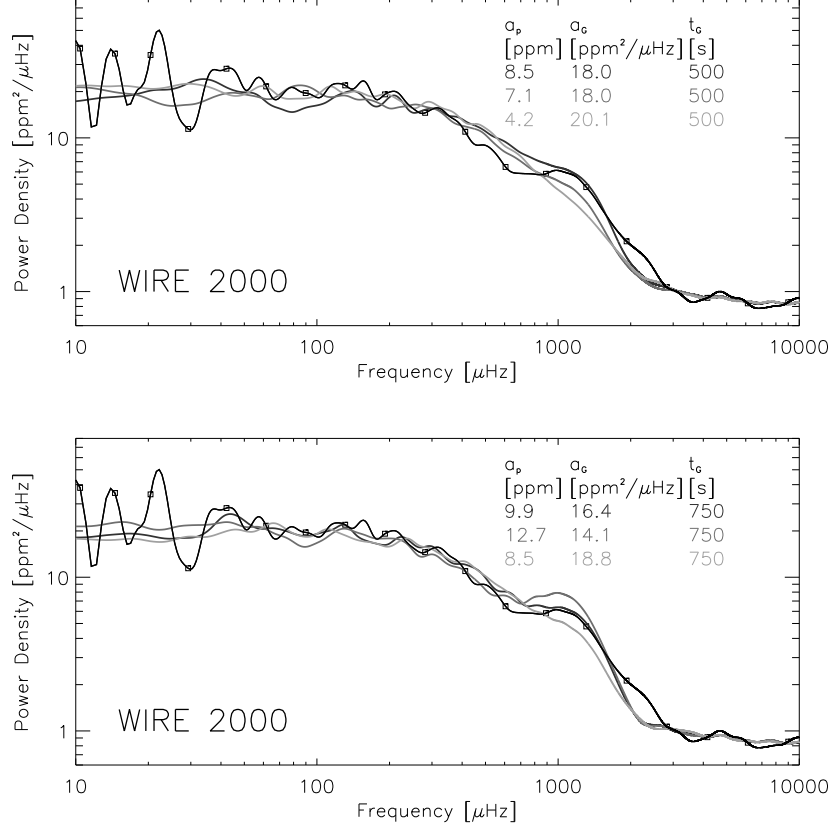


Fig. 9.— The power density spectra of the WIRE 2000 light curve compared to models with granulation timescales of 500 (*upper* panel) and 750 seconds. The WIRE 2000 spectrum is marked by open box symbols. The different shades of gray correspond to the filled circles on the contour plot in Fig. 8. The parameters of the models are given in the upper right corner of each panel.

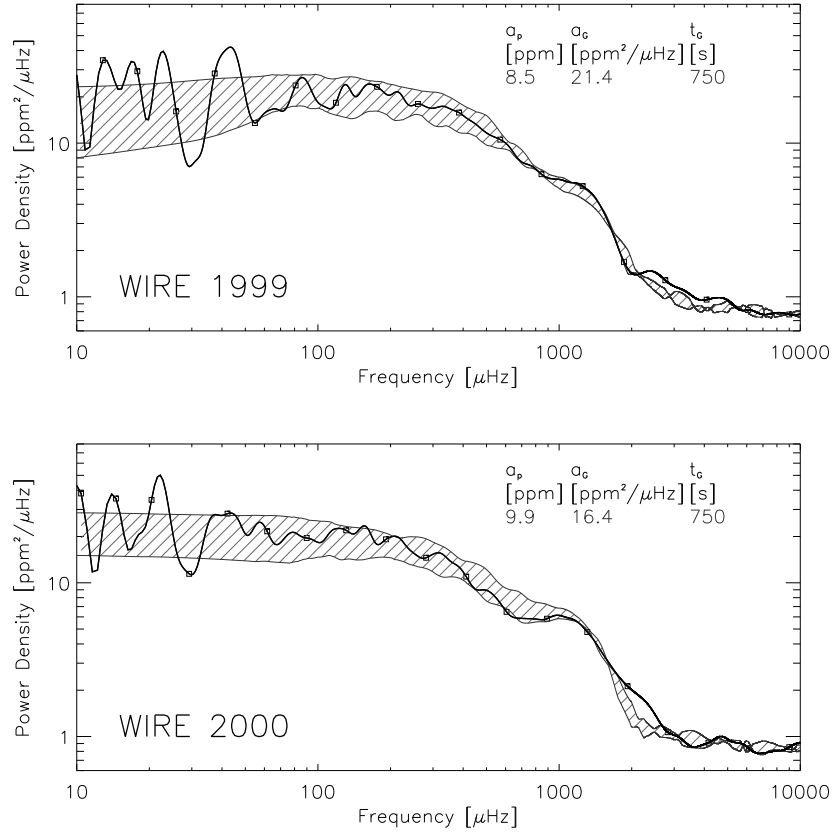


Fig. 10.— The power density spectra of the WIRE 1999 (*upper* panel) and WIRE 2000 light curves and the models with the best fit. The WIRE spectra are marked by open box symbols and the $1\text{-}\sigma$ variation of the simulations is shown by the hatched region.

To put further constraints on the granulation PD and oscillation amplitudes, we have computed a large grid of simulations that include the ranges of parameters indicated above. We made time series with granulation timescales of 500, 750, 1000, and 1250 s; granulation PD in the range 12–41 $\text{ppm}^2/\mu\text{Hz}$ in average step size of 3 $\text{ppm}^2/\mu\text{Hz}$; and oscillation amplitudes between 0 and 13 ppm in steps of 1.5 ppm. The white noise was fixed at 100 and 105 ppm for the WIRE 1999 and 2000 time series, respectively. Each time series was calculated for five different random number seeds to estimate the scatter. In total we calculated $5 \times 440 = 2200$ time series for both the WIRE 1999 and 2000 datasets.

For each time series we calculated the power density spectrum. In order to select the best models we computed the χ^2 in the frequency range between 50 and 5000 μHz . We used logarithmic frequency bins in order to avoid giving too much weight to the high-frequency part of the spectrum.

In Fig. 8 we show results for the simulations of the WIRE 2000 time series. The two contour plots correspond to granulation timescales of 500 and 750 s, respectively. The contours show the χ^2 value for each set of granulation PD and oscillation amplitudes. The crosses mark the locations of the computed simulations. We have marked three models with circles of different color that have the smallest values of χ^2 , and the corresponding power density spectra are shown in Fig. 9, where the simulation parameters are given in each panel. We find that the region 400–800 μHz is better fitted for the granulation timescale of 750 s. This region is located just below the excess power seen around 1 mHz.

In Fig. 10 we show examples of simulations that provide good fits to the WIRE 1999 and 2000 power density spectra. The hatched regions correspond to the $1\text{-}\sigma$ uncertainty, based on the scatter of the five simulations with different random number seeds. The agreement between 1999 and 2000 for the best-fitting parameters is not surprising given the similarity of the power density curves (cf. Fig. 5). The main difference between the two WIRE PDS is the region 400–800 μHz . As noted in Sec. 2, we found a group of data points that were offset from the rest in the WIRE 1999 light curve that may be the source of additional noise.

We thus conclude that the parameters that best fit the observed power density curves lie in the range 750 ± 200 , 18 ± 4 $\text{ppm}^2/\mu\text{Hz}$, and 8.5 ± 2 ppm for the granulation timescale, granulation PD and p-mode amplitude, respectively.

The granulation time scale in Procyon is about twice that of the Sun (VIRGO data; cf. Fig. 5), the granulation PD is three times higher, and the peak p-mode amplitude is twice solar.

4.3. Peak height distribution

Following Bedding et al. (2005), we have investigated whether the distribution of peak heights in the power density spectrum of the WIRE light curves (cf. Fig. 4) agrees with the simulations. We consider the frequency range 700–1 800 μHz , which contains the excess power that may be due to oscillations. Since the power increases rapidly when going to lower frequencies, we have normalized the power density spectrum as illustrated in Fig. 11. We did this by removing the overall slope by dividing the PDS by the straight line shown in the logarithmic plot in Fig. 11. We have chosen a simulation of the WIRE 2000 time series with granulation timescale and granulation PD of 750 s and 16.4 $\text{ppm}^2/\mu\text{Hz}$, respectively, which gave the best fit for the PDS (cf. Fig. 10). The p mode peak amplitude is 9.9 ppm and the lifetime of the modes is 1 day. The solid line was divided into the spectrum and the result is shown as the insert in Fig. 11. The same was done for the observed power density spectrum.

In Fig. 12 we show the cumulative distribution of peak heights after this normalization, i.e. the fraction of peaks that are above a given level. The cut-off at around $N_{\text{above}}/N_{\text{total}} \simeq 0.0005$ corresponds to the inverse of the number of data points in the spectrum in the frequency range 700–1 800 μHz , i.e.. we have $N_{\text{total}} = 1\,865$. The light gray lines are results for 100 simulations of pure white noise, while the dark gray lines are based on 100 simulations of granulation and p-modes with the same parameters used for Fig. 11. We conclude that the actual WIRE data from 2000 contains an excess of strong peaks which is consistent with p-modes. The WIRE 1999 data set gives very similar results.

4.4. Search for a Comb-like Structure

The p-modes detected in the Sun and other solar-like stars show a distinct distribution of peaks, often referred to as the comb structure. The separation between the dominant peaks is twice the large separation and can be determined from the autocorrelation of the power spectrum. We applied this method to the WIRE data but did not find evidence for the large separation. We applied the same analysis to the simulations with the parameters found in Sect. 4.2, also with a negative result. We repeated the analysis for a simulation with the same duration and time sampling but with a 100% duty cycle and did indeed recover the input for the large separation. However, the S/N was also improved significantly since there was about five times more data points in this simulation. This emphasizes that a high duty cycle is important when future asteroseismology space missions will observe solar-like stars.

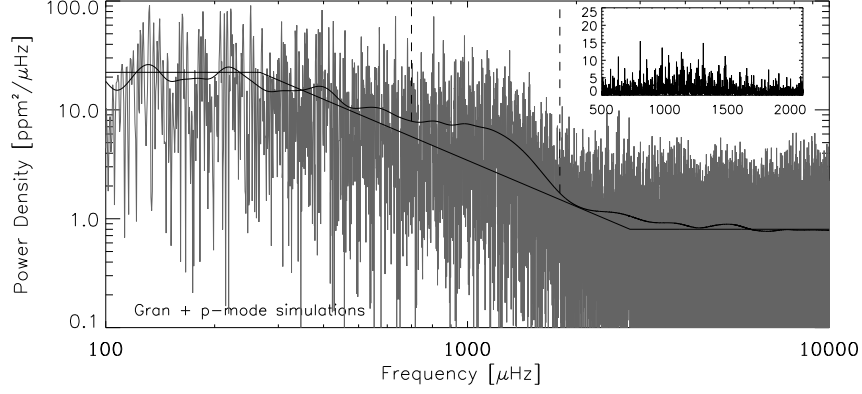


Fig. 11.— Power density spectrum for one of the simulations of granulation and p-modes when using the same input times as for the WIRE 2000 time series. The solid line marks the normalization and the resulting spectrum is shown in the insert. The dashed lines mark the frequency region used for the examination of the peak distribution (cf. Fig. 12).

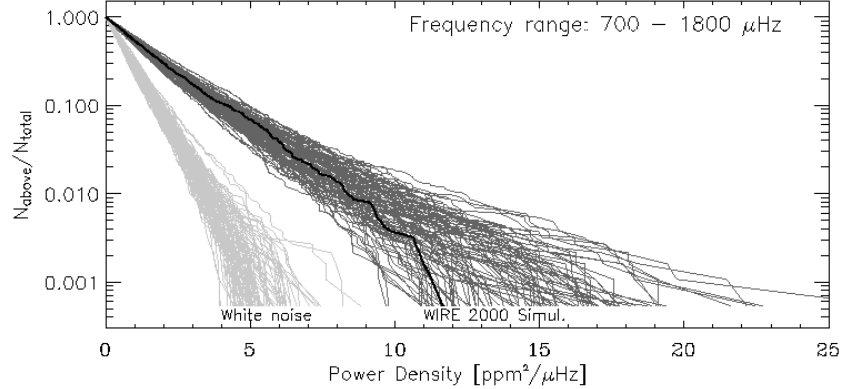


Fig. 12.— The cumulative distribution of peak heights in the observed WIRE 2000 light curve (single black curve). The light gray lines are simulations of white noise while the dark gray lines simulations of granulation and p modes.

5. Conclusion

We have analyzed light curves of Procyon from the WIRE satellite from two epochs in 1999 and 2000. When comparing the power density spectrum (PDS) of Procyon and the Sun we find a higher noise level by a factor of 1.8 ± 0.3 at frequencies in the range 100–300 μHz , which is expected since Procyon is hotter and more luminous than the Sun.

We find evidence for excess power around 1 μHz which is consistent with the p-modes reported from spectroscopic campaigns (Brown et al. 1991; Martić et al. 2004; Eggenberger et al. 2004; Claudi et al. 2005). We have compared the observed PDS of the observations with a grid of simulations with different input granulation timescale, granulation PD and p-mode amplitude. We have thus constrained the granulation timescale, granulation PD and p-mode amplitude to be 750 ± 200 , $18 \pm 4 \text{ ppm}^2/\mu\text{Hz}$, and $8.5 \pm 2 \text{ ppm}$, respectively. The upper limit we put on the p-mode peak amplitude is consistent with measured radial velocity amplitudes which lie in the range 50–70 cm/s (Martić et al. 2004). We note that the determined peak amplitude of the p-modes does not depend on the assumed life time (1 day) but will depend slightly on our assumed distribution of peaks (cf. Fig. 6). In particular this is true for the assumed width of the the Gaussian envelope used for modifying the input peak heights.

We have compared the distribution of peak heights in the PDS of the observations and in several simulations of granulation and p-modes. We find a good agreement for the peak distribution which supports our interpretation of the excess power around 1 μHz as being due to p-modes. However, we find no evidence for the comb-like structure expected for solar-like oscillations.

Our results do not agree with the much higher noise level (a factor two in amplitude) found from observations with the MOST satellite (Matthews et al. 2004). The analysis by Bedding et al. (2005) of the MOST power spectrum showed that the the distribution of peak heights was not consistent with a pure noise source and Bedding et al. (2005) concluded that an additional error source could be present. This is confirmed by the present comparison with observations from the WIRE satellite.

HB and DLB acknowledge support from NASA (NAG5-9318) and from the US Air Force Academy. HB and HK are grateful for the support from the Danish Research Council (Forskningsråd for Natur og Univers) and TRB thanks the Australian Research Council. We are grateful to the MOST team for making the Procyon data available through the Canadian Astronomy Data Centre (operated by the Herzberg Institute of Astrophysics, National Research Council of Canada). We also thank Dennis Stello for useful discussions

and, in particular, his ideas for the investigation of the peak-height distribution in power spectra.

REFERENCES

- Aigrain, S., Favata, F. & Gilmore, G., 2004, Proc. 2nd Eddington workshop, ESA SP-538, eds. F. Favata & S. Aigrain, p. 215
- Bedding, T. R., Kjeldsen, H., Butler, P. R., McCarthy, C., Marcy, G.W., 2004, ApJ, 614, 380
- Bedding, T. R., Kjeldsen, H., Bouchy, F. et al., 2005, A&A, 432, 43L
- Brown, T. M., Gilliland, R. L., Noyes, R. W. & Ramset, L. W., 1991, ApJ, 368, 599
- Buzasi, D. L., Catanzarite, J., Laher, R. et al., 2000, ApJ, 532, 133
- Buzasi, D. L., Bruntt, H., Bedding, T. R., et al., 2004, ApJ, 619, 1072
- Claudi, R. U., Bonanno, A., Ventura, R. et al., 2005, A&A, 429, L17
- Eggenberger, P., Carrier, F., Bouchy, F. & Blecha, A., 2004, A&A, 422, 247
- Fröhlich, C., Andersen, B.N., Appourchaux, T., Berthomieu, G., 1997, Sol. Phys., 170, 1
- Harvey J.W., 1985, In: Noyes R.W., Rhodes E.J. Jr. (eds.) Probing the depths of a Star: the study of solar oscillations from space. JPL 400-327
- Kjeldsen, H., Bedding, T. R., Frandsen, S., & Dall, T. H., 1999, MNRAS, 303, 579.
- Martic, M., Lebrun, J.-C., Appourchaux, T. & Korzennik, S.G., 2004, A&A, 418, 295
- Matthews, J. M., Kusching, R., Guenter, D. B. et al., 2004, Nature, 430, 51, Erratum: 430, 921
- Pallé, P.L., Roca Cortes, T. & Jimenez, A., 1999, ASP Conf. Ser., 173, 297
- Retter, A., Bedding, T.R., Buzasi, D.L. et al., 2003, ApJ, 591, 151
- Rucinski, S. M., 2004, Walker, G. A. H., Matthews, J. M., et al., 2004, PASP, 116, 1093
- Schou, J. & Buzasi, D.L., 2001, Proc. SOHO 10/GONG 2000 Workshop, ESA SP-464, p. 391

Stello, D., Kjeldsen, H., Bedding, T.R., et al., 2004, Sol. Phys., 220, 207

Stetson, P. B, 1990, PASP, 102, 932

Walker, G., Matthews, J., Kusching, R. et al., 2003, PASP, 115, 1023